*Chinese Science Bulletin* 2004 Vol. 49 Supp. I 50—59

# Simulation experiments on secondary thermal stress of biodegraded bituminous sandstones

GONG Se[1,2], PENG Ping'an[1], LU Yuhong[3], XIAO Zhongyao[3], JIA Wanglu[1], WANG Zhenqi[1], YU Chiling[1], LIU Dehan[1], LU Jialan[1] & LIU Jinzhong[1]

1. State Key Laboratory of Organic Geochemistry, Chinese Academy of Sciences, Guangzhou Institute of Geochemistry, Guangzhou 510640, China;
2. Graduate School of the Chinese Academy of Sciences, Beijing 100039, China;
3. Tarim Oilfield of China National Petroleum Corporation, Kuerle 841000, China

Correspondence should be addressed to Peng Ping'an (e-mail: pinganp@gig.ac.cn)

**Abstract** **Secondary variation of reservoir is a hot problem in petroleum geochemistry field. Several kinds of secondary variations have taken place after the formation of bituminous sandstones in the Tarim Basin including biodegradation, washing, dissipation and secondary thermal stress. Biodegraded bituminous sandstones were used in the experiment. Pyrolysis experiment has been performed in a closed system, simulating secondary thermal stress with continual burial of Silurian bituminous sandstones which may cause the changes in molecular compositions, carbon isotope and physical properties of bituminous sandstones. The results are as follows: (i) Gases are mainly product during the experiment and carbon isotope of gas is lighter. (ii) Yield of $C_{6+}$ hydrocarbon is relative smaller, and yielded oil is mainly light oil. (iii) Chromatogram character of biodegraded oil-sand is similar to that of saturated hydrocarbon in extracts from present-day bituminous sandstones. (iv) Porosity of bituminous sandstones gradually increases with increasing temperature. Fluorescence color of bituminous sandstones gradually become darker. Reflected light color of bitumen in bituminous sandstones becomes darker with increasing temperature and reflectivity of bitumen increases with increase in temperature. It is speculated that secondary thermal stress has great effect on molecular composition and structure of bituminous sandstones.**

**Keywords: bituminous sandstones, thermal simulation, thermal stress, biodegradation, secondary variation.**

**DOI: 10.1360/04wd0348**

At present, reservoir secondary variation is more concerned by petroleum geologists. Generally, reservoir secondary variations include biodegradation, water washing, oxidation, migration diffusion and thermal alteration. There are extensive literatures reporting the effects on crude oils in reservoir caused by reservoir secondary variation which can change component, carbon isotope and physical character of oil in reservoir[1—6]. Water washing can lead to increase of crude oil solidifying point[7]. Crude oil can be changed into heavy oil through washing, biodegradation, oxidation and diffusion of light hydrocarbon[8]. In addition oxidation of oil can lead to decrease of paraffin content and increase of oil density, sulfur content, acidity and viscosity which have huge negative economy consequence on oil production and refining operations[1]. Another reservoir secondary variation hardly paid attention to by geologist is secondary thermal stress of biodegraded reservoir due to increase of burial depth. Basins containing oil and gas in the west of China basically belong to superimposed basin[9,10] and have undergone multi-generation tectonism. Biodegraded reservoir generally regenerated hydrocarbon with increase of burial depth[11, 12]. Probe on the composition and carbon isotope of reservoir and the problem of regeneration hydrocarbon is important to whether exploration or development of oil and gas.

The Silurian hydrocarbon reservoir in the Tarim Basin formed at late Caledonian, and immediately after the accumulation, the hydrocarbon reservoir was uplift to the earth surface and destroyed by heavy biodegradation, then large-scale area bituminous sandstones came into being[13,14]. In the later endless geological time, bituminous sandstones forming at early stage perhaps have undergone thermal maturation with increase of burial depth and recharge of subsequent oil. Several studies about Silurian bituminous sandstones genesis have been carried out[15,16] but the regeneration hydrocarbon has paid no attention to by petroleum geologists. How are molecular composition and structure of bituminous sandstones changed with increase of burial depth? Have regeneration hydrocarbon taken place? Those are problems concerned by geologists. Pyrolysis experiment has been carried out in a closed system to simulate thermal maturation with continual sedimentation of Silurian bituminous sandstones.

## 1 Sample and method

(i) Sample. Sample in well Tazhong117 (TZ117, 4438.8 m) was selected from Silurian bituminous sandstones in Tazhong District of the Tarim Basin which represent the sample undergoing thermal maturation again after initial biodegradation and water washing. In contrast, the other sample in well Zhengxie41 (ZX41, 1262.5 m) was selected from Tertiary oil-sand in Zhengjia District of Shengli Oilfield which represent the sample only suffering biodegradation and water washing. Pyrolysis simulation experiment has been performed in a closed system to simulate secondary thermal stress with continual burial of Silurian bituminous sandstones. Block and powder samples are made for each sample. Block samples are used to study organic petrography and powder samples are used to carry out organic geochemistry analysis.

(ii) Method. Samples were sealed into gold tubes

under inert gases, then these gold tubes were placed in autoclave in which some water was added to produce needed pressure, and then the autoclave was placed in the oven. Heating 72 h at each temperature, the autoclave was removed from the oven. Three parallel gold tubes put into the oven were used to make organic petrology and the following organic geochemical analysis.

(1) Gas chromatography. Gas composition analysis was performed by Agilent HP6890N GC-FID. GC conditions: Paraplot Q capillary column (50 m×0.50 mm). The temperature program used was isothermal for 2 min at 70℃, programmed at 20℃/min to 180℃ and then isothermal at 180℃ for 10 min. Organic and inorganic gas can be examined simultaneously through FID and ECD detector in this 6890N GC. Nitrogen was used as the carrier gas. The temperature of FID detector was 180℃. External standard method was applied to quantify the gas composition.

GC analyses of saturated hydrocarbon, aromatic hydrocarbon and lighter hydrocarbon were performed by Agilent HP6890 GC-FID. GC conditions of saturated hydrocarbon: DB-5 capillary column (30 m×0.32 mm). The temperature program was isothermal 2 min at 80℃, programmed at 4℃/min to 290℃ and then isothermal at 290℃ for 30 min. Nitrogen was used as the carrier gas. The temperature of FID detector was 290℃. GC conditions of aromatic hydrocarbon were the same with saturated hydrocarbon except that programmed at 3℃/min to 290℃. Only the temperature program of lighter hydrocarbon was different from saturated hydrocarbon which was isothermal 5 min at 35℃, programmed at 4℃/min to 290℃, then isothermal for 40 min. The weighing was used for the quantification of heavy hydrocarbon($C_{15+}$). Internal standard ($C_{20}D_{42}$) method was applied to quantify the lighter hydrocarbon ($nC_6$—$nC_{14}$) and *n*-alkane in saturated hydrocarbon.

(2) Gas chromatography-mass spectrometry (GC-MS). GC-MS analyses of saturated hydrocarbon and aromatic hydrocarbon were performed on a Voyager mass spectrometry coupled to a Finnigan $8000^{top}$ gas chromatography. Fused silica capillary column (60 m× 0.32 mm) of DB-5 was used. The temperature program was the same as GC conditions. Helium was used as the carrier gas. The transfer line temperature was 250℃, the ion source temperature was 250℃ and the ion source was operated in the electron impact (EI) mode at 70 eV.

(3) Gas chromatography-isotope ratio mass spectrometry. Gas composition carbon isotope was analyzed by Isochrom HP5890 GC/IRMS. Analysis conditions: Paraplot Q capillary column (30 m×0.32 mm). The temperature program: isothermal for 3 min at 50℃, programmed at 25℃/min to 180℃ and then isothermal at 180℃ for 8 min. Helium was used as the carrier gas.

Carbon isotope composition of individual *n*-alkanes was performed on Finnigan Delta $plus^{XL}$ system interfaced to a HP6890 GC. Analysis conditions: DB-5 Fused silica capillary column (30 m×0.32 mm). The temperature program was isothermal for 1 min at 60℃, programmed at 8 ℃/min to 150℃, then isothermal for 1 min at 150℃, and then programmed at 3℃/min to 290℃, isothermal for 15 min at 290℃. Helium was used as the carrier gas. The temperature of gasifying room was 300℃.

## 2 Results

( i ) Changes in composition and carbon isotope of pyrolysate from biodegraded oil-sand in well ZX41.

(1) Gas, light hydrocarbon and heavy hydrocarbon. Methane is mainly gaseous product during thermal simulation and increases continually as thermal stress increases (Table 1). The $C_{2-5}$ gas yield reaches a maximum at 550℃. Total gas yield takes on an obviously climbing trend after 400℃ (Fig. 1). Gas wetness is higher constantly and remains larger than 45% before 600℃, then reaches a minimum of 26% at 600℃ (Fig. 2).

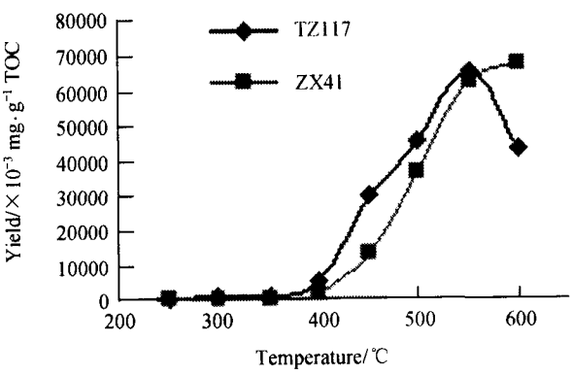


Fig. 1. Changes in total gas yield ($C_1$—$C_5$) with increasing temperature.

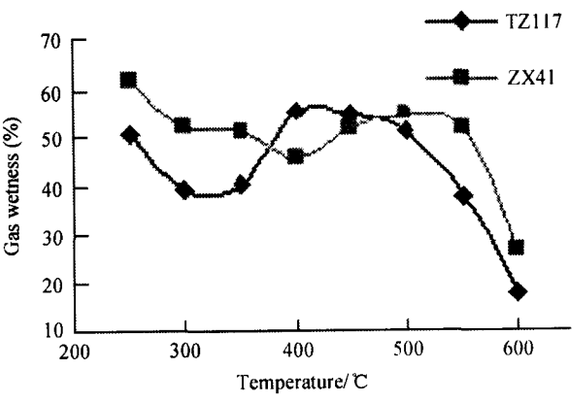


Fig. 2. Changes in gas wetness with increasing temperature.

Table 1 Changes in cracked products and saturated hydrocarbon parameters during pyrolysis at various temperatures

| Well 77℃ | TZ117 (4438.8 m) | | | | | | | | ZX41 (1262.5 m) | | | | | | | |
|---|---|---|---|---|---|---|---|---|---|---|---|---|---|---|---|---|
| | unheated | 250 | 300 | 350 | 400 | 450 | 500 | 550 | 600 | 250 | 300 | 350 | 400 | 450 | 500 | 550 | 600 |
| $C_1/\times10^{-3}$mg·g$^{-1}$ TOC | | 109.7 | 249.1 | 489.8 | 1539.4 | 9576.4 | 16067.6 | 37416.7 | 42796.2 | 3.3 | 49.0 | 75.4 | 629.6 | 4510.6 | 11233.8 | 22720.2 | 54122.4 |
| $C_{2-5}/\times10^{-3}$ mg·g$^{-1}$ TOC[a)] | | 112.8 | 162.1 | 331.3 | 1924.6 | 11584.7 | 17001.9 | 22869.8 | 9427.1 | 5.4 | 54.3 | 79.2 | 539.2 | 4815.3 | 13736.4 | 24333.1 | 19639.6 |
| $C_{6-14}$/mg·g$^{-1}$ TOC[b)] | | 3.1 | 3.3 | 2.6 | 5.0 | 15.5 | 18.3 | 10.0 | 4.9 | 0.6 | 0.8 | 0.5 | 1.1 | 3.3 | 6.0 | 2.5 | 0.3 |
| $C_{15+}$/mg·g$^{-1}$ TOC[c)] | | 262.0 | 254.6 | 215.3 | 188.2 | 71.0 | 22.4 | 9.1 | 8.8 | 157.2 | 190.1 | 150.1 | 112.0 | 96.8 | 38.8 | 8.4 | 4.5 |
| Total/mg·g$^{-1}$TOC[d)] | | 265.3 | 258.3 | 218.7 | 196.7 | 107.7 | 73.8 | 79.4 | 65.9 | 157.8 | 191.0 | 150.8 | 114.3 | 109.4 | 69.8 | 58.0 | 78.6 |
| Saturates (%)[e)] | | 42.29 | 15.90 | 26.69 | 27.59 | 43.41 | 27.22 | – | – | 23.73 | 18.05 | 32.59 | 34.98 | 10.55 | 38.04 | – | – |
| Aromatics (%)[e)] | | 30.47 | 26.94 | 38.78 | 33.11 | 33.95 | 59.17 | – | – | 23.27 | 27.23 | 32.55 | 26.40 | 42.15 | 50.18 | – | – |
| Nonhydrocarbon+ Aaphaltene (%)[e)] | | 27.24 | 57.15 | 34.53 | 39.3 | 22.63 | 13.61 | – | – | 53.00 | 54.72 | 34.86 | 38.62 | 47.32 | 11.79 | – | – |
| *n*-Alkane /μg·g$^{-1}$ sample | | 25.19 | 8.26 | 8.83 | 10.05 | 14.21 | 2.73 | – | – | 4.09 | 2.21 | 7.23 | 43.69 | 38.16 | 26.29 | – | – |
| Gas wetness (%)[f)] | | 50.7 | 39.4 | 40.4 | 55.6 | 54.7 | 51.4 | 37.9 | 18.1 | 62.1 | 52.6 | 51.2 | 46.1 | 51.6 | 55.0 | 51.7 | 26.6 |
| Dry coefficient (%)[g)] | | 49.3 | 60.6 | 59.6 | 44.4 | 45.3 | 48.6 | 62.1 | 81.9 | 37.9 | 47.4 | 48.8 | 53.9 | 48.4 | 45.0 | 48.3 | 73.4 |
| *n*-Alkane carbon Number range | $C_{14}$—$C_{34}$ | $C_{15}$—$C_{36}$ | $C_{15}$—$C_{35}$ | $C_{15}$—$C_{35}$ | $C_{15}$—$C_{35}$ | $C_{15}$—$C_{35}$ | $C_{15}$—$C_{32}$ | – | – | – | – | – | $C_{14}$—$C_{33}$ | $C_{14}$—$C_{34}$ | $C_{14}$—$C_{34}$ | – | – |
| *n*-Alkane maxima | $C_{19-20}$ | $C_{20}$ | | $C_{19-20}$ | $C_{19}$ | $C_{18-19}$ | $C_{18}$ | – | – | – | – | – | $C_{17}$ | $C_{17-20}$ | $C_{17-18}$ | – | – |
| CPI[h)] | 1.05 | 0.97 | 1.11 | 0.96 | 1.01 | 1.10 | 1.08 | – | – | – | – | – | 1.12 | 1.21 | 1.06 | – | – |
| Ph/$C_{18}$ | 0.48 | 0.40 | 0.40 | 0.38 | 0.36 | 0.15 | – | – | – | – | – | – | 3.35 | 0.55 | 0.07 | – | – |
| $nC_{21}^{-}$ / $nC_{22}^{+}$ | 0.91 | 0.87 | 0.87 | 0.93 | 0.75 | 1.39 | 2.31 | – | – | – | – | – | 0.84 | 1.11 | 5.12 | – | – |

a) Sum of *n*-alkane and *i*-alkane; b) includes compounds between *n*C6 and *n*C14; c) includes saturates, aromatics, nonhydrocarbon and asphaltene; d) Total=Methane+$C_{2-5}$+ $C_{6-14}$+ $C_{15+}$; e) precent of group composition; f) area ratio between $C_2$—$C_5$ and total gas; g) area ratio between methane and total gas; h) CPI=[$\Sigma C_{25}$—$C_{33}$ (odd)/$\Sigma C_{24}$—$C_{32}$(even)+$\Sigma C_{25}$—$C_{33}$(odd)/$\Sigma C_{26}$—$C_{34}$(even)]/2; i) area ratio between $nC_{15}$—$nC_{21}$ and $nC_{22+}$; –, lower content of heavy hydrocarbon (C15+) lead to some parameters uncaculating, and so are not listed here.

Light hydrocarbon yield in pyrolysate increases gradually with temperature increasing, and reaches a maximum of 6.0 mg/g TOC at 500℃ (Table 1, Fig. 3). Heavy hydrocarbon ($C_{15+}$) yield in pyrolysate increases gradually at 250℃—500℃ and decreases continually when the content of *n*-alkane reaches a maximum of 1060.4 μg/g TOC. Saturated hydrocarbons have a slight odd-even *n*-alkane predominance at 400℃—500℃ and the $CPI_{24\text{-}43}$ values are between 1.06 and 1.21. Ph/$nC_{18}$ ratio decreases with increasing temperature.

Relative amounts of saturated hydrocarbon biomarkers and mature-related parameters show little variation with increasing temperature and while relative amounts of alkylnaphthalenes and alkylphenanthrenes in aromatic hydrocarbon vary obviously with increasing temperature and the methylphenanthrene index increases evidently.

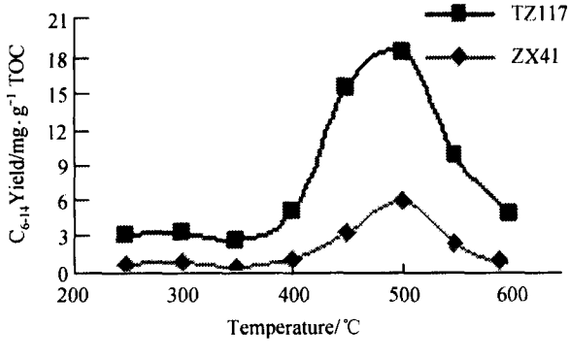


Fig. 3. Production curve of light hydrocarbon with increasing temperature.

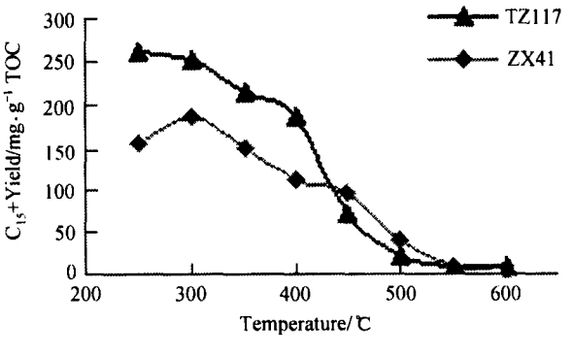


Fig. 4. Production curve of heavy ($C_{15+}$) hydrocarbon with increasing temperature.

(2) $C_{1-4}$ hydrocarbon gas and individual *n*-alkane carbon isotopes. $C_1$—$C_4$ specific carbon isotopes take on two trends with increasing temperature (Fig. 5). $\delta^{13}C_1$ values become heavier as temperature increases, while $\delta^{13}C_{2-4}$ values become lighter firstly as temperature increases and later heavier again, such that $\delta^{13}C_2$ value decreases from −31.74‰ at 400℃ to −35.12‰ at 500℃ and later increases to −27.93‰ at 600℃. Above phenomenon is found in many literatures[17, 18]. The reason occurring this phenomenon may be due to heterogeneity of organic matter or various kinds of chemical bonds. Different chemical bonds have different characters at different energy levels and so different fractionation of carbon isotope exists. Heterogeneity of organic matter in lower mature sample is more obvious which is just consistent with maturity character of well ZX41[1]. The magnitude of difference between $\delta^{13}C_{ethane}$ and $\delta^{13}C_{propane}$ increases from 0.66 to 14.88 with increasing temperature (Fig. 6) which is similar to the described for high maturity hydrocarbon gases by Ronald et al.[19].

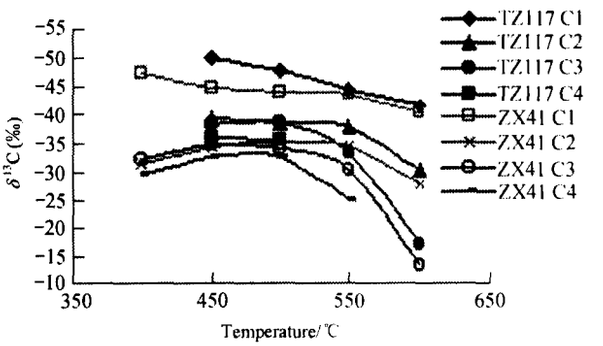


Fig. 5. Carbon isotope of gas composition of samples in wells TZ117 and ZX41.

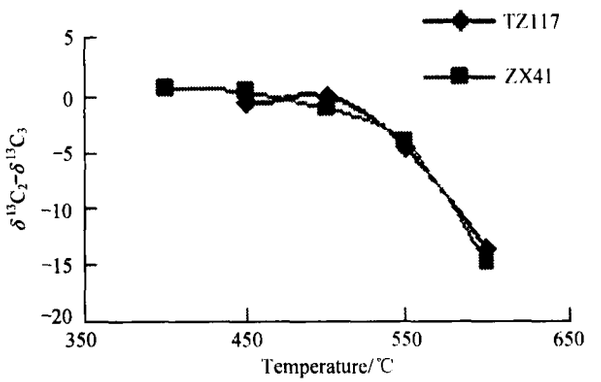


Fig. 6. Changes in the difference between $\delta^{13}C_{ethane}$ and $\delta^{13}C_{propane}$ with increasing temperature.

Only few samples in higher temperature contain abundant *n*-alkane due to heavy biodegradation of well ZX41. Carbon isotopes of individual *n*-alkane in pyrolys-

1) Wangzhenqi, Study on Genesis Mechanism Heavy Oil in Zhengjia-Wangzhuang Oilfield, Jiyang Depression, Chinese Academy of Sciences, Guangzhou Institute of Geochemistry, 2004.

ate at 400℃ and 450℃ were analyzed (Fig. 7). Carbon isotope value of individual *n*-alkane is between −28.71‰ and −27.47‰ (the average value is −28.34‰) at 450℃, and carbon isotope value of individual *n*-alkane is between −28.64‰ and −25.65‰ (the average value is −26.34‰) at 500℃. Increase of carbon isotope of individual *n*-alkanes is about 2‰ from 450℃ to 500℃ which shows that carbon isotope is more influenced by maturity. Carbon isotope of asphaltene in extracts of well ZX41 oil-sand is −26.13‰ which is close to carbon isotope of individual *n*-alkane at 550℃.

Table 2 Carbon isotope of gas composition at different temperature

| Well and depth | *T*/℃ | $\delta^{13}C_1$(‰) | $\delta^{13}C_2$(‰) | $\delta^{13}C_3$(‰) | $\delta^{13}C_4$(‰) |
|---|---|---|---|---|---|
| TZ117 4438.8 m | 400 | −49.20 | −45.40 | −37.65 | |
| | 450 | −50.27 | −39.26 | −38.44 | −35.92 |
| | 500 | −48.03 | −38.80 | −38.69 | −35.74 |
| | 550 | −44.70 | −38.01 | −33.50 | |
| | 600 | −41.64 | −30.61 | −16.92 | |
| ZX41 1262.5 m | 400 | −47.74 | −31.74 | −32.40 | −29.62 |
| | 450 | −45.01 | −34.50 | −35.07 | −32.69 |
| | 500 | −44.17 | −35.12 | −34.03 | −32.55 |
| | 550 | −44.02 | −34.40 | −30.42 | −24.95 |
| | 600 | −40.35 | −27.93 | −13.06 | |

(ii) Changes in composition and carbon isotope of pyrolysate from bituminous sandstones in well TZ117

(1) Gas, light hydrocarbon and heavy hydrocarbon. Methane is still the main gaseous product in pyrolysate from bituminous sandstones in well TZ117 though bituminous sandstones have undergone various kinds of secondary variations. Changes in every gas composition yield are similar to well ZX41. Total gas yield produced by bituminous sandstones in well TZ117 is not lower than that in well ZX41 until 550℃ (Fig. 1). Gas wetness decreases at lower temperature (250℃—300℃), and later increases at higher temperature (350℃—400℃), and then decreases again with increasing temperature. Gas wetness remains larger than 40% until 550℃ and reaches a minimum of 18.1% (Fig. 2). Light hydrocarbon yield increases continually with increasing temperature and reaches a maximum of 18.3 mg/g TOC at 500℃ (Table 1, Fig. 3). The $C_{15+}$ yield decreases gradually as temperature increases (Talbe 1, Fig. 4) and at the same time carbon number range distribution reduces gradually and maximum carbon number becomes smaller also. Odd-even predominance is not obvious between 250℃ and 500℃and $CPI_{24\text{-}34}$ value is about 1. Ph/$nC_{18}$ ratio takes on a decreasing trend with increasing temperature. Variation trend of saturated hydrocarbon biomarkers and aromatic hydrocarbon biomarkers in pyrolysate of bituminous sandstones in well TZ117 is similar to that in well ZX41.

(2) Carbon isotope of $C_{1\text{-}4}$ hydrocarbon gas and individual *n*-alkane. Gas carbon isotope values at 400℃ can be regarded as reference because of less gas yield. Carbon isotopes of $C_{1\text{-}4}$ hydrocarbon gas tend to become heavier gradually with increasing temperature (Fig. 5), and especially, $\delta^{13}C_2$ and $\delta^{13}C_3$ value changes evidently between 550℃ and 600℃. $\delta^{13}C_2$ value increases from −38.01‰ at 550℃ to −30.61‰ at 600℃. $\delta^{13}C_3$ value increases from −33.50‰ at 550℃ to −16.92‰ at 600℃. Correlation of $\delta^{13}C_{ethane} - \delta^{13}C_{propane}$ and temperature (Fig. 6) shows that the absolute value of $\delta^{13}C_{ethane} - \delta^{13}C_{propane}$ decreases firstly and later increases at higher temperature which is slightly different from the previous work[19].

Carbon isotopes of individual *n*-alkane in pyrolysate from bituminous sandstones in well TZ117 are shown in Fig. 7. Carbon isotope value of individual *n*-alkane is between −34.46‰ and −33.61‰ (the average value is −34.00‰) at 250 ℃, and between −34.00‰ and −33.37‰ (the average value is −33.73‰) at 450℃. Little difference at various temperature exists with increasing temperature except that carbon isotope of higher carbon number *n*-alkane at 300℃ is slight lighter. Carbon isotope of asphaltene in extracts of well TZ117 oil-sand is −32.84‰, which is heavier than individual *n*-alkane.

(iii) Influence on bituminous sandstones structure and character of bitumen by secondary thermal stress. Changes in structure of oil-sand in well ZX41 are not observed for oil-sand is loose. Only fluorescence color at different temperature is observed. Fluorescence color of bituminous sandstones is yellow at lower temperature and becomes Kelly and then green with increasing temperature. Until 550℃—600℃, no fluorescence color emits. Fluorescence color at different temperature of bituminous sandstones in well TZ117 is similar to that in well ZX41. Bitumen color of bituminous sandstones in well TZ117 varies from brown to hoar under reflected light microscopy with increasing temperature and the reflectivity of bitumen increases with increasing temperature.

Changes in structure and color of bituminous sandstones in well TZ117 observed by reflected light through stereomicroscope are shown in Fig. 8. Color of pre-pyrolysis sample is buff. Quartz grains are wrapped by oil-like bitumen and not only small pores but also most of large pores are all filled. This phenomenon shows that Silurian bituminous sandstones perhaps have undergone hydrocarbon regeneration or charge of sequential oil in geological time. Color of sample becomes darker gradually with increasing temperature. Unfilled pores become more and more till 450℃ which indicates that high molecular weight hydrocarbons have cracked to form gas. Color of sample changes into puce at 600℃, and many small unfilled pores are observed when gasification is very obvious. This phenomenon is consistent with the fact that gas

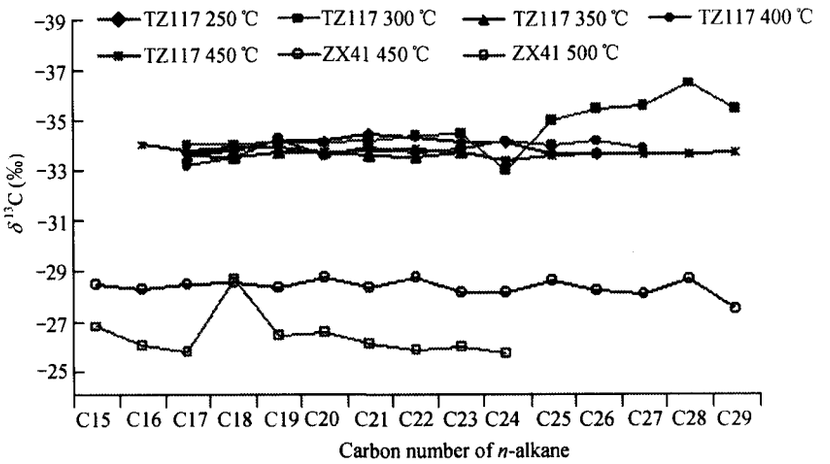


Fig. 7. Changes in carbon isotope of individual *n*-alkane with increasing temperature. Carbon isotope of asphaltene, well TZ117: −32.84‰; well ZX41: −26.13‰.

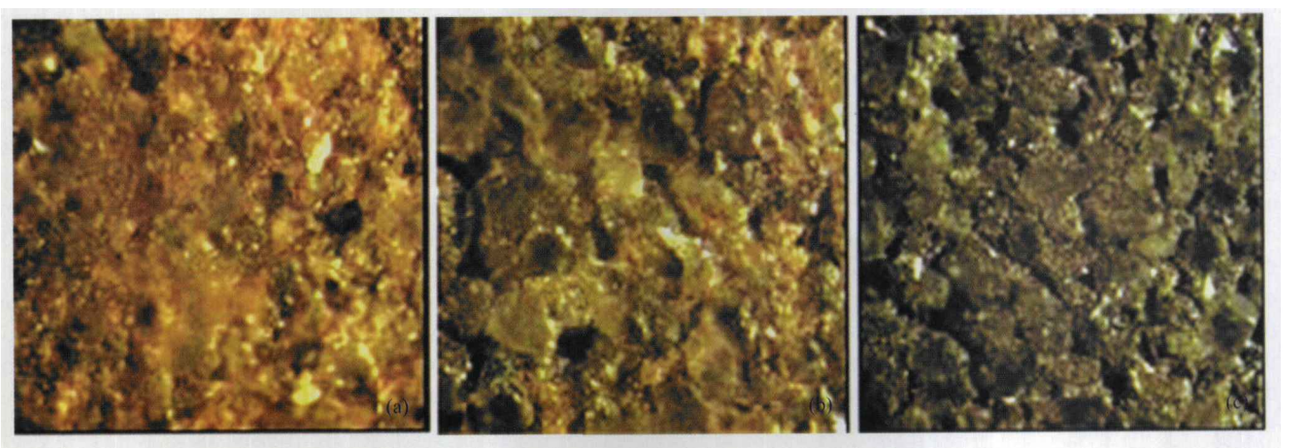


Fig. 8. Changes in structure and color of bituminous sandstones in well TZ117 observed by reflected light.

yield increases abruptly after 400℃.

## 3 Discussion

( i ) Effect on composition and carbon isotope of organic matter in bituminous sandstones caused by secondary thermal stress. Methane yield of samples in wells TZ117 and ZX41 increases continually with increasing temperature, and this is the same with the previous publications[17,18,20,21]. The reason is that $C_{2+}$ hydrocarbons can crack to form methane. Total gas yield is lower at 250℃—400℃, and increases quickly after 400℃(Fig. 1). Because of its higher maturity, total gas yield of Silurian bituminous sandstones reaches a maximum at 550℃. Simulation experiment on oil-sand explains that secondary pyrolysis for biodegraded bituminous sandstones can take place due to subsequent thermal stress and produces a large number of natural gas. There is possibility for Silurian bituminous sandstones formed at late Caledonian to crack again due to resediment of formation, producing natural gas.

Gas wetness of cracking gas for oil-sand in well ZX41 is higher than that of well TZ117 (Fig. 2). Two reasons may be included: one is that the maturity of oil-sand in well ZX41 is lower, and the other is different H-rich extent in extracts of two samples which is due to that drier gases are thought to be generated from H-poor organic matter while wetter gases are generated from H-rich organic matter[22,23]. It is well known that the gas generated during artificial maturation in spite of using open systems or close systems is much wetter than natural gas of thermogenic origin[24−28]. In this experiment, the dry coefficient of gas is 37%—82% (Table 1) and much lower than that of secondary crude oil cracking gas in partial gas field in the Tarim Basin. For example, dry coefficient of natural gas in Hetianhe Gasfield is 96%—99%.

Heavy hydrocarbon yield decreases continually with increasing temperature (Fig. 3). This indicates that there is little possibility for bituminous sandstones to produce heavy oils during secondary cracking. Moreover the $nC_{21}^{-}/nC_{22}^{+}$ ratios for well ZX41 are all much larger than 1 which shows that middle-low molecular weight compounds are the main products in $C_{15+}$ heavy hydrocarbon. Yield of light hydrocarbon and gas increases gradually with increasing temperature and reaches maximums at 500℃ and 550℃ respectively. These phenomena prove that thermal stress can lead to obvious changes of organic matter in bituminous sandstones.

Decrease of $Ph/C_{18}$ ratios for biodegraded oil-sand in well ZX41 and bituminous sandstones in well TZ117 is consistent with crude oil cracking results for Ronald et al.[19] and demonstrates that branched alkanes are less stable than *n*-alkanes. Subsequent thermal stress has no obvious effect on saturated hydrocarbon, while has obvious influence on aromatic hydrocarbon especially for alkylnaphthalenes and alkylphenanthrenes.

Several publications show that $\delta^{13}C_1$ value coming from geological section tends to become heavier with increasing thermal evolution[29—31]. Results in this experiment are consistent with the publications. The difference of carbon isotope between two temperature points increases with increasing temperature which reflects that carbon isotope fractionation of crude oil cracking gas is obvious and so our results confirm that $\delta^{13}C_1$ value of crude oil cracking gas in the Tarim Basin is lighter than that of pyrolytic gas originated from kerogen[32]. Carbon isotope of gas composition from bituminous sandstones during the thermal simulating experiment tends to become heavier and moreover takes on the feature of positive sequence of carbon isotope. Carbon isotope of gas composition from oil-sand in well ZX41 shows partial opposite sequence at 400℃—450℃, that is to say $\delta^{13}C_1 < \delta^{13}C_2 > \delta^{13}C_3 < \delta^{13}C_4$, and this phenomenon also occurred during thermal simulation of hydrocarbon source rock[33]. The difference of carbon isotope between ethane and propane ($\delta^{13}C_2 - \delta^{13}C_3$) has been used as a maturity indicator[34,35]. For a type II kerogen, Lorant et al.[35] showed that in open system pyrolysis, the difference between $\delta^{13}C_{ethane}$ and $\delta^{13}C_{propane}$ decreases with increasing temperature, while in closed system pyrolysis, the difference between $\delta^{13}C_{ethane}$ and $\delta^{13}C_{propane}$ increases with increasing temperature. It is suggested that system openness must be considered to interpret maturity of natural gas using carbon isotope. Oil cracking results in Ronald et al.[19] also confirmed this point. In this experiment, the difference between $\delta^{13}C_{ethane}$ and $\delta^{13}C_{propane}$ in well ZX41 increases with increasing temperature, but as to sample in well TZ117, the difference between $\delta^{13}C_{ethane}$ and $\delta^{13}C_{propane}$ decreases from 450℃ to 500℃ and then increases gradually at 500℃—600℃. Carbon isotope of gas composition in pyrolysates from oil-sand in well ZX41 is heavier than that of well TZ117 at each corresponding temperature which may be due to different sources and maturities of organic matter in two samples.

When oil/gas source, depositional environment and maturity of hydrocarbon source rock are similar, carbon isotope of crude oil and its group composition and kerogen keeps to the following law: saturated hydrocarbon < crude oil < aromatic hydrocarbon < nonhydrocarbon < asphaltene < kerogen. Extracts carbon isotope of hydrocarbon source rock is heavier than that of corresponding crude oil but lighter than that of asphaltene in crude oil and kerogen[36]. In this experiment, carbon isotope of individual *n*-alkane in pyrolysate from wells ZX41 and TZ117 is lighter than that of corresponding asphaltene which shows that source of pyrolysate is consistent with asphaltene. Wang Darui[37] performed the studies on stratigraphy and geochemistry of marine carbonate rocks in the Tarim Basin. He thought carbon isotope of marine carbonate rocks of Middle-Upper Ordovician relative to Lower Ordovician has obvious positive anomaly and the maximum anomaly value reaches 3‰. Zhao Mengjun[38] acknowledged that carbon isotope of crude oil source from Lower Ordovician or more deeper strata is generally lighter than −32‰. Carbon isotope of individual *n*-alkane in pyrolysate from bituminous sandstones in well TZ117 is lighter than −33‰ and also accords with the law that carbon isotope of saturated hydrocarbon is lighter than that of asphaltene. Carbon isotope of asphaltene in extracts from bituminous sandstones represents the carbon isotope of crude oil which sourced from hydrocarbon source rock of Cambrian-Lower Ordovician and formed reservoir at Caledonian. If the large amounts of *n*-alkane in extracts from well TZ117 come from the charge of subsequent oil, the carbon isotope of *n*-alkane would depart from the value of −34‰—−33‰. Hence it is considered that the large amounts of *n*-alkane in extracts from well TZ117 come from the hydrocarbon produced by secondary cracking of bituminous sandstones due to secondary thermal stress but do not exclude charge of subsequent oils. Carbon isotope of individual *n*-alkane is mainly influenced by hydrocarbon source and also influenced by maturity at the same time. Carbon isotopes of asphaltene (−32.84‰) in extracts and individual *n*-alkane (−33.62‰—−34.62‰) in pyrolysate from well TZ117 are lighter, showing that the hydrocarbon source is marine organic matter, while carbon isotopes of asphaltene (−26.13‰) in extracts and individual *n*-alkane (−26.34‰—−28.3‰) in pyrolysate from well ZX41 are heavier, showing that the hydrocarbon source is lacustrine organic matter. Carbon isotopes of individual *n*-alkane from bituminous sandstones in well TZ117 at different temperature show no

obvious changes. The difference of carbon isotope of individual *n*-alkane in pyrolysate from well ZX41 reaches 2‰ between 450℃ and 500℃ which shows the carbon isotope of individual *n*-alkane in well ZX41 is more influenced by maturity. It may be related to the maturity of hydrocarbon source rock. Maturity of organic matter in oil-sand from well ZX41 is lower, and strong heterogeneity of organic matter and various kinds of chemical bonds in sample may result in obvious fractionation of carbon isotope with increasing temperature. Higher maturity of organic matter in bituminous sandstones from well TZ117, weaker heterogeneity of organic matter and few kinds of chemical bonds in sample may lead to little fractionation of carbon isotope with increasing temperature.

(ii) Regeneration hydrocarbon of bituminous sandstones caused by secondary thermal stress. At present, two kinds of viewpoints are used to explain the source of soluble hydrocarbons in Silurian bituminous sandstones: (1) soluble hydrocarbons may source from regeneration hydrocarbon produced by biodegraded bituminous sandstones due to strara resediment; (2) soluble hydrocarbons may source from recharge of subsequent oils[14]. Large-scale area bituminous sandstones distributing in Tazhong and Tabei area in the Tarim Basin contain higher organic matter content. If the process of regeneration hydrocarbon existed, the process discharging hydrocarbon would have occurred at Tertiary which helps to accumulate and preserve oil and gas; hence Silurian bituminous sandstones may be important hydrocarbon source rock in the Tarim Basin. Chromatograms of saturated hydrocarbon in pyrolysate from oil sandstones in well ZX41 at different temperature are shown in Fig. 9. Chromatogram of saturated hydrocarbon at 350℃ still takes on a feature of biodegradation and no *n*-alkane occurs. Chromatogram of saturated hydrocarbon at 400℃ shows few *n*-alkanes occurring. Chromatogram of saturated hydrocarbon at 450℃ shows a complete *n*-alkane distribution which is similar to chromatogram character of saturated hydrocarbon in extracts from present-day bituminous sandstones. Hence it is speculated that Silurian bituminous sandstones formed at late Caledonian can regenerate hydrocarbon during secondary thermal stress. Chromatograms of saturated hydrocarbon in well ZX41 and well TZ117 tend to similarity with increasing temperature. Chromatograms of saturated hydrocarbon in low mature Shengli biodegraded oil-sand explain that it is obvious for subsequent thermal stress to alter Silurian bituminous sandstones in the Tarim Basin. Yields of gas, light hydrocarbon and heavy hydrocarbon also indicate that subsequent thermal stress can make large-scale area bituminous sandstones regenerate oil, but mainly light oil.

The phenomenon of bituminous sandstones and hoar sandstones alternating layers exists in Tazhong and Tabei area in the Tarim Basin. Physical property of bituminous sandstones is well, for example the average porosity in well Tazhong37 is 16.3%. Physical property of sandstones

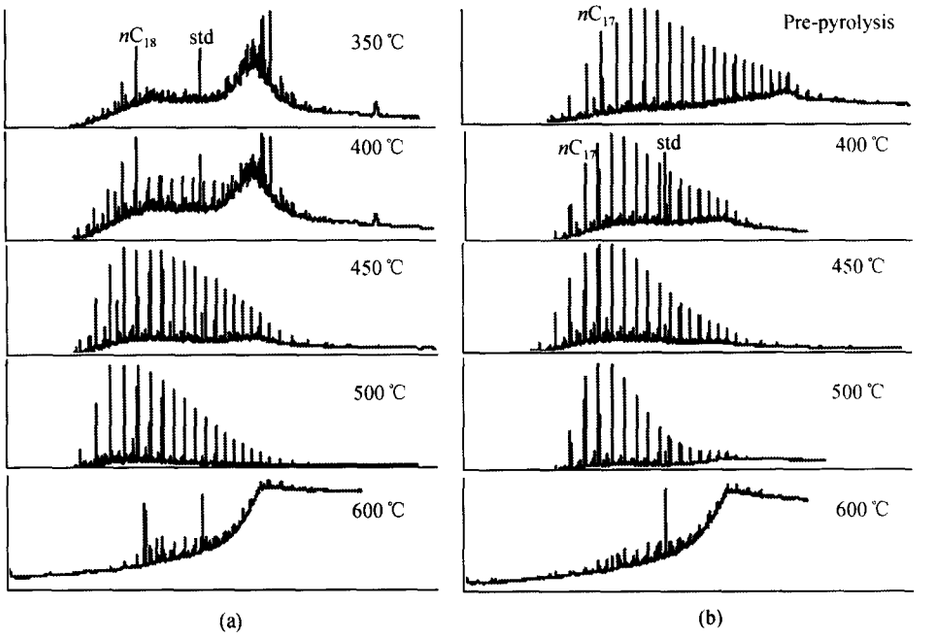


Fig. 9. Chromatograms of saturated hydrocarbon in extract of samples in wells ZX41(a) and TZ117(b) at different temperature and pre-sample in well TZ117. std represents the internal standard $C_{24}D_{50}$.

without bitumen is not well, and the average porosity in well Tazhong37 is only 11.8%. Well Ha1 and well Ha4 in Tabei area have the same phenomenon. Sandstones containing bitumen are medium-fine sand and siltstones do not contain bitumen[39]. In this experiment, the phenomenon of increase in porosity which is due to organic matter in bituminous sandstones changing into gas may indicate that regeneration hydrocarbon caused by secondary thermal stress can lead to porosity increasing. Therefore high porosity of sandstones containing bitumen in Tazhong and Tabei area may show that bituminous sandstones have regenerated hydrocarbon due to secondary thermal stress. In addition, Liu[15] determined the bitumen reflectance in water immersion ($R_W$1.35%—1.53%) which is in accord with the country rock. This shows that Silurian bituminous sandstones have ever undergone strong thermal stress so that large amounts of hydrocarbons were produced and accordingly higher bitumen reflectance can occur.

## 4 Conclusion

Gases are the main product during secondary thermal stress of Silurian bituminous sandstone. Large amounts of gases are produced after 400℃ which shows that bituminous sandstones can produce large amounts of natural gas by secondary cracking. Hence bituminous sandstones in the Tarim Basin may be gas potential source rock. Seen from the yeild of light hydrocarbon and heavy hydrocarbon, subsequent thermal stress can make large-scale area bituminous sandstones regenerate oil, but mainly light oil.

Comparing with natural gas in Tazhong district, carbon isotope of gas pyrolyzed by bituminous sandstone is lighter. Carbon isotope of ethane to propane in wells TZ117 and ZX41 shows different trends which may be related to source and maturity of samples. Comparing with carbon isotope of asphaltene, carbon isotope of individual *n*-alkane shows that large amounts of *n*-alkane occurring in bituminous sandstones may be owing to hydrocarbon regeneration resulted from secondary thermal stress.

Saturated hydrocarbon biomarkers show no obvious changes with increasing temperature while the aromatic maturity ratio, for example the methylphenanthrene index, increases abruptly with the increasing temperature.

Secondary thermal stress can lead to porosity increase and so higher porosity of sandstones containing bitumen in the Tarim Basin may be the result of hydrocarbon regeneration. As thermal stress increasing, fluorescence color of bituminous sandstones changes from yellow to Kelly, green and black.

Secondary thermal stress can change the composition, carbon isotope and structure of bituminous sandstones. Hydrocarbon regeneration will not form large-scale crude oil but light oil and gas.

**Acknowledgements** This work was part of the project "Studies on correlation of different oil-gas source and petroleum accumulation geochronology in superimposed basin in China" and the authors appreciate the generous financial support of this work by the "973" Project in China (Grant No. 1999043308).

## References

1. Connan, J., Biodegradation of crude oils in reservoir, Advances in Petroleum Geochemistry (Brooks, J., Welte, D. H. eds.), London: Academic Press, 1984, 229—335.
2. Palmer, S. E., Effects of biodegradation and water washing on crude oils composition, Organic Geochemistry, Principals and Applications (Engel, M. H., Macko, S. A. eds.), New York: Plenum, 1993, 511—533.
3. Clay, E. R., Michael, M., Jeremy, D., The controls on biodegradation in the San Joaquin Valley, AAPG Bulletin, 1997, 81(4): 682.
4. George, S. C., Boreham, C. J., Minifie, S. A., The effect of minor to moderate biodegradation on $C_5$ to $C_9$ hydrocarbons in crude oils, Organic Geochemistry, 2002, 33(12): 1293—1317.
5. Larter, S., The control on the composition of biodegraded oils in the deep subsurface——part 1: biodegradation rates in petroleum reservoirs, Organic Geochemistry, 2003, 34(4): 601—613.
6. Hwang, R. J., Baskin, D. K., Reservoir connectivity and oil homogeneity in a large-scale reservoir, Middle East Petroleum Geoscience, 1994, 2: 529—541.
7. Xu Zhiming, Wang Tingdong, Jiang Ping et al., Probe on the water washing and higher solidifying point crude oil, Geochimica (in Chinese), 2000, 29(6): 556—561.
8. Dou Lirong, Yang Tao, Origin of heavy oils at Jirgalangtu depression of Erlian Basin, Oil &Gas Geology (in Chinese), 1995, 16(4): 324—330.
9. Wang Qingchen, Jin Zhijun, Superimposed basin and oil-gas formation and accumulation. China Basic Science (in Chinese), 2002, 6(4): 4—7.
10. Zhao Wenzhi, Zhang Guangya, Wang Hongjun et al., Basic features of petroluem geology in the superimposed petroliferous basin of China and their research methodologies, Petroleum Exploration and Development (in Chinese), 2003, 30(2): 1—8.
11. Lin Qing, Wang Peirong, Jin Xiaohui et al., Reservoir forming history of Ordovician reservoir at well Tzhong45 in the north slope of Tazhong uplift, Petroleum Exploration and Development (in Chinese), 2002, 29(3): 5—7
12. Xu Shiqi, Conditions of forming reservoir in Sinian Cambrain of Caledonian ancient uplift, Natural Gas Industry (in Chinese), 1999, 19(6): 7—10.
13. Liu Luofu, Zhao Jianzhang, Zhang Shuichang et al., Hydrocarbon filling ages and evolution of the Silurian asphalt sandstones in the Tarim basin, Acta Sedimentologica Sinica (in Chinese), 2000, 18(3): 475—479.
14. Li Yuping, Wang Yong, Sun Yushan et al., Two accumulation stages of the Silurian hydrocarbon reservoirs in central area of the Tarim

Basin, Chinese Journal of Geology (in Chinese), 2002, 37(Supp.): 45—50.
15. Liu Dameng, Jin Kuili, Wang Lingzhi, Characteristics and genesis of Silurian bituminous sandstones in the Tarim Basin, Geoscience (in Chinese), 1999, 13(2): 169—175.
16. Liu Luofu, Zhao Jianzhang, Zhang Shuichang et al., Genetic types and characteristics of the Silurian asphalt sandstones in the Tarim Basin, Acta Petrolei Sinica (in Chinese), 2000, 21(6):12—17.
17. Wang Zhaoyun, Cheng Keming, Zhang Baisheng, Study on the characteristics and evolution regularity of product of gas under pyrolysis simulation experiments, Petroleum Exploration and Development (in Chinese), 1995, 22(3): 36—40.
18. Michels, R., Elie, M., Laurence, M. et al., Understanding of reservoir gas compositions in a natural case using stepwise semi-open artificial maturation, Marine and Petroleum Geology, 2002, 19(5): 589—599.
19. Ronald, J. H., Yongchun, T., Isaac, R. K., Insight into oil cracking based on laboratory experiment, Organic Geochemistry, 2003, 34(12): 1651—1672.
20. Wang Zhenping, Fu Xiaotai, Lu Shuangfang et al., An analogue experiment of gas generation by crude oil cracking, characters of products and its significances, Natural Gas Industry (in Chinese), 2001, 21(3): 12—15.
21. Feng Zihui, Chi Yuanlin, Du Hongwen et al., Carbon isotopic composition and yield of Gaseous hydrocarbon by oil hydrous pyrolysis in rock medium, Acta Sedimentologica Sinica (in Chinese), 2002, 20(3): 505—509.
22. Price, L. C., Scholl, M., Constraints on the orgins of hydrocarbon gas from compositions of gases at their site of origin, Nature, 1995, 378(23): 368—371.
23. Schaefer, R. G., Galushkin, Y. I., Kolloff, A. et al., Reaction kinetics of gas generation in selected source rocks of the West Siberian Basin: implication for the mass balance of early-thermogenic methane, Chemical Geology, 1999,156(1-4): 41—65.
24. Mango, F. D., The light hydrocarbon in petroleum: a critical review, Organic Geochemistry, 1997, 26(7-8): 417—440.
25. Mango, F. D., Methane concentration in natural gas: the genetic implications, Organic Geochemistry, 2001, 32(10): 1283—1287.
26. Behar, F., Vandenbroucke, M., Teerman, S. C. et al., Experimental simulation of gas generation from coals and a marine kerogen, Chemical Geology, 1995, 126(3-4): 247—260.
27. Behar, F., Vandenbroucke, M., Tang, Y. et al., Thermal cracking of kerogen in open and closed systems: determination of kinetic parameters and stoichiometric coefficients for oil and gas generation, Organic Geochemistry, 1997, 26(5-6): 321—339.
28. Snowdon, L. R., Natural gas composition in a geological environment and the implication of the process of generation and preservation, Organic Geochemistry, 2001, 32(7): 913—931.
29. Stahl, W. J., Carbon isotope fractionation in natural gases, Nature, 1974, 251: 134—135.
30. Dai Jinxing, Qi Houfa, Song Ya et al., On the indications for identifying gas from oil and gas from coal measure, Acta Petrolei Sinica (in Chinese), 1985, 6(2): 31—38.
31. Xu Yongchang, Shen Ping, A preliminary study on geochemical characteristics of coal- type gas in Zhongyuan-Huabei oil-gas area, Acta Sedimentologica Sinica (in Chinese), 1985, 3(2): 37—45.
32. Zhao Mengjun, Zeng Fangang, Qin Shengfei et al., Two pyrolytic gases found and proved in the Tarim Basin, Natural Gas Industry (in Chinese), 2001, 21(1): 35—38.
33. Zheng Jianjing, Thermal simulation research of partial opposites sequence of carbon isotope and ethane carbon isotope of gases, Acta Sedimentologica Sinica (in Chinese), 1999, 17(Supp.): 811—814.
34. James, A. T., Correlation of reservoired gases using the carbon isotopic composition of wet gas components, American Association of Petroleum Geologists Bulletin, 1990, 74(9): 1441—1458.
35. Lorant, F., Prinzhofer, A., Behar, F. et al., Carbon isotopic and molecular constraints on the formation and the expulsion of thermogenic hydrocarbon gases, Chemical Geology, 1998, 147(3-4): 249—264.
36. Li Meijun, Wang Yanshan, Wang Tieling et al., The characteristics of carbon isotope composition of the Dongbu depression in the Liaohe Basin, Geoscience, 2003, 17(2): 217—221.
37. Wang Darui, Bai Yulei, Jia Chengzao, The petroleum geological significance of carbon isotopic positive anomaly of the Middle-Upper Ordovician in the Tarim Basin, northwest China, Petroleum Exploration and Development (in Chinese), 1998, 25(4): 15—16.
38. Zhao Mengjun, Liao Zhiqin, Huang Difan et al., Several aspects on hydrocarbon generation of the Ordovician source base on petroleum geochemical features, Acta Sedimentologica Sinica (in Chinese), 1997, 15(4): 72—96.
39. Liu Luofu, Zhao Jianzhang, Zhang Shuichang et al., The depositional and structural settings and the bituminous sandstones distribution characters of the Silurian in the Tarim Basin, Acta Petrolei Sinica (in Chinese), 2001, 22(6): 11—17.

(Received August 5, 2004; accepted October 22, 2004)